Using Zeolite-Zirconia-Copper Nanocomposites as a New Asphaltene Inhibitor for Improving Permeability Reduction during CO 2 Flooding

Mohsen Mansouri
Ilam University
Yaser Ahmadi (yaser.ahmadi@ilam.ac.ir)
Ilam University

Research Article

Keywords: Nanoparticles, asphaltene, zeolite, Zirconia, Copper

Posted Date: December 16th, 2021

DOI: https://doi.org/10.21203/rs.3.rs-1138220/v1

Using Zeolite-Zirconia-Copper Nanocomposites as a New Asphaltene Inhibitor for Improving Permeability Reduction during CO_2 Flooding

Mohsen Mansouri[1], Yaser Ahmadi[1*]

[1] Chemical and Petroleum Engineering Department, Ilam University, P.O. Box 69315/516, Ilam, Iran

Abstract

Using nanoparticles for adsorbing asphaltene was known as an efficient method among researchers for crude oil upgrading and in this study, Zeolite-zirconia-copper nanocomposites (NCs) has been synthesized and characterized with SEM, XRD, BET, and EDX for asphaltene precipitation inhibition in the static phase and solving asphaltene deposition problems of dynamic CO_2 flooding in low permeability carbonate reservoir. CO_2-oil IFT tests, isotherm models, natural depletion tests at static phase were performed in the presence of NCs and the results were compared with zeolite nanoparticles. Then, CO_2 core flooding tests at dynamic phase were designed in the presence of NCs at obtained static conditions for surveying permeability/porosity reduction in porous media. After adding NCs and zeolite nanoparticles, the 2nd to 1st slope ratio in CO_2-oil IFT tests increased from 19.697 % to 20.895 % and 29.851 %, respectively which shows NCs adsorbed more asphaltene in comparison to zeolite nanoparticles which confirmed UV-Vis results. NCs was decreased asphaltene precipitation more than zeolite at same points during natural depletion tests and it was selected for dynamic CO_2 tests. After adding NCs, asphaltene depositions which occurs after CO_2 injection was decreased and permeability/porosity reduction parameters were improved.

Keywords: Nanoparticles, asphaltene, zeolite, Zirconia, Copper

*Corresponding's author E-mail: yaser.ahmadi@ilam.ac.ir

1. Introduction

Asphaltene precipitation is one of the main concern during oil production, and changing thermodynamic conditions such as pressure, composition and temperature were known as important factors for asphaltene precipitation [1-2]. Asphaltenes are insoluble in paraffins (heptane and pentane) and soluble in aromatics (toluene) [3-5]. During oil production, problem occurs in the presence of asphaltene particles such as plugging due to precipitating of this solid phase in crude oil [6-7]. Researchers introduced many methods for solving asphaltene precipitation problems such as treatments with mechanical approaches or adding solvents and surfactants while due to specific characteristics of nanoparticles, using nanoparticles especially nanocopmosite was introduced as an efficient method among different researchers [8-15]. The main parameter in their study is asphaltene adsorption on nanoparticles surface which is depends on many factors such as carboxlic, pyrrolic, Pyridinic existence in asphaltene, type and nanoparticles characteristics, and nanoparticles-asphaltene interactions [16-25]. Various nanoparticles such as zeolite and metal oxides and zirconia find applications in different fields such as catalysis and adsorption [26-31]. Zeolites are known as a reliable adsorbent of asphaltene, and hydrated aluminosilicate is the most important parts of zeloites [26-27], and these nanoparticles used as support materials for stabilizing nano particles to produce high efficacy nanocomposites [32-34]. Hosseinpour et al., shows that zirconia samples with surface acid sites has high BET specific surface area values in compared to other nanoparticles such as Fe_2O_3, NiO, and WO_3 which shows strength of interactions between the asphaltenes and this sample [28]. Another nanoparticles which are widely used due to their availability and low cost is copper oxide nanoparticles. Copper oxide has a wide variety of applications including efficient adsorbent [35 40], foam stabilization [41], EOR [42], and environmental remediation [43].

Changing composition due to adding CO_2 gas was known as a main concern in porous media, and it was found that asphaltene deposition especially at inlet part of core caused formation damage which should be fully considered [44]. Moreover, it was found that agglomeration problem relevant to nanoparticles can be solved with using nanocomposites [45]. In this study, Zeolite-zirconia-copper oxide nanocopmosites (NCs) was used for surveying asphaltene adsorption on the surface and removal of asphaltene as an asphaltene inhibitor and the results compared with zeolite nanoparticles as a reference. As NCs had better results in the static phase and was selected for performing dynamic CO_2 tests. Although the application of zeolite, zirconia, copper oxide at different cases were surveyed in previous studies such as asphaltene adsorption, introducing NCs as a possible asphaltene adsorbent and dynamic CO_2 tests were not covered according to our knowledge. At first phase, adsorption behavior during CO_2-oil IFT tests was observed and results was matched with real natural depletion tests in the presence of NCs and zeolite nanoparticles. Natural depletion was used as the main sources of making asphaltene precipitation by changing pressures and the main points in natural depletion tests were selected based on the CO_2-oil interfacial tension (IFT) tests (higher adsorption potential points). Two tests of CO_2-oil interfacial tension (IFT) and Ultraviolet–visible spectroscopy (UV-Vis) spectrophotometer were used for describing asphaltene adsorption on the nanoparticles surface, and two different isotherm models of Langmuir and Freundlich were completely surveyed in the presence of NCs and zeolite nanoparticles. Finally, based on the static phase results, NCs was selected for performing dynamic CO_2 tests and improving permeability reduction/porosity reduction parameters.

2 Materials and Methodology

2.1 Materials

Crude oil was collected from one of Iranian oil reservoir in the west with oil density of 0.864 g/cm^3 and viscosity of 9.9 cP at 40 °C. Table 1 shows reservoir oil composition and the results of saturate-aromatic-resin-asphaltene (SARA) test was shown in Figure 1.

Table 1. Reservoir oil composition.

Components	Reservoir oil (Mole %)	Components	Reservoir oil (Mole %)
N_2	0.08	nC_4	5.77
CO_2	0.56	iC_5	3.7
C_1	3.44	nC_5	5.3
C_2	1.88	C_6	5.92
C_3	3.45	C_{7+}	68.67

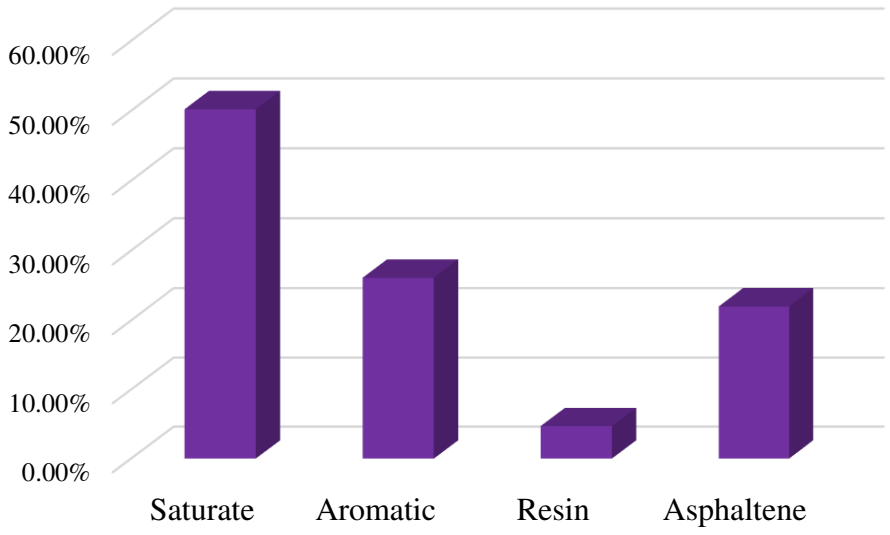

Figure 1. SARA test results.

Gas and brine permeability and porosity results and other specific of carbonate plug which was used in dynamic CO_2 test were shown in Table 2.

Table 2. Properties of plug for performing dynamic CO_2 tests.

Properties	Carbonate plug
Length (cm)	4.80
Diameter (cm)	3.55
Gas pore volume (cc)	10.02
Gas permeability (cc)	8.43
Gas porosity (%)	17.30
Brine pore volume (cc)	11.10
Brine porosity (%)	19.47
Brine permeability (mD)	0.15

For extracting asphaltenes, standard IP143 method was used [46], and normal heptane 99%, toluene 99%, ethanol 99 %and Watson paper grade 42 with a thickness of 0.22 micrometer were prepared from Merck brand.

2.2 Methodology

2.2.1 Synthesis of zeolite nanoparticles

For preparing eolite, below 7 steps were performed:

1. Preparing the gel with the percentage molar of Al_2O_3: 46 SiO_2: 2.7 TPA: 5 Na_2O: 1.3 Trien: 2500 H_2O.

2. Pouring the prepaid gel into a Teflon autoclave chamber (up to volume of 70%).

3. Placing autoclave in a temperature-controlled set up for 72 hours.

4. Cooling the autoclave and removing the products.

5. Washing the product with water (up to pH = 7).

6. Drying the resulting powder at 100 °C for 12 hours.

7. Calcined the product at 550 °C for 8 hours.

2.2.2 Synthesis of Zeolite-Zirconia-Copper oxide Nanocomposites

Below main steps were used for synthesis of NCs

1. Dissolving $ZrCl_4$ in 50 ml propanol and obtaining Na-ZSM-5 zeolite gel.
2. Adding 5 ml (%30 v/v) H_2O_2 o the solution.
3. Setting the pH of Zirconia gel solution at 9.
4. Preparing ZSM-5 with dissolving zeolite powder and $Cu(NO_3)_3.6H_2O$ in water
5. Setting the pH of green obtained solution at 9 with adding ten milliliter NH_3.
6. Obtaining NCs with adding ZSM-5:ZrO_2:CuO = 70:25:5, respectively.
7. Stirring and aging of the obtained NCs for two days.
8. Performing filteration and cacination process at 300°C for three hours.

2.2.3 Interfacial tension (IFT) tests

CO_2-Oil interfacial tension tests were performed with experimental set up as Figure 2. This set up can measured interfacial tension at specific pressure and temperature.

IFT set up contained different parts such as high pressure dioxide carbon cylinder, high pressure and high temperature cells, pumps for injecting the crude oil, pressure gauges, temperature sensor, and data acquisition software. Four steps were used for obtaining CO_2-oil IFT as:

1. Using Nitrogen for flushing the lines and main cell.
2. Injecting dioxide carbon gas through the main cell.
3. Pumped the oil (or oil with NCs) for obtaining oil droplets as Figure 2.
4. Using software for IFT measurements.

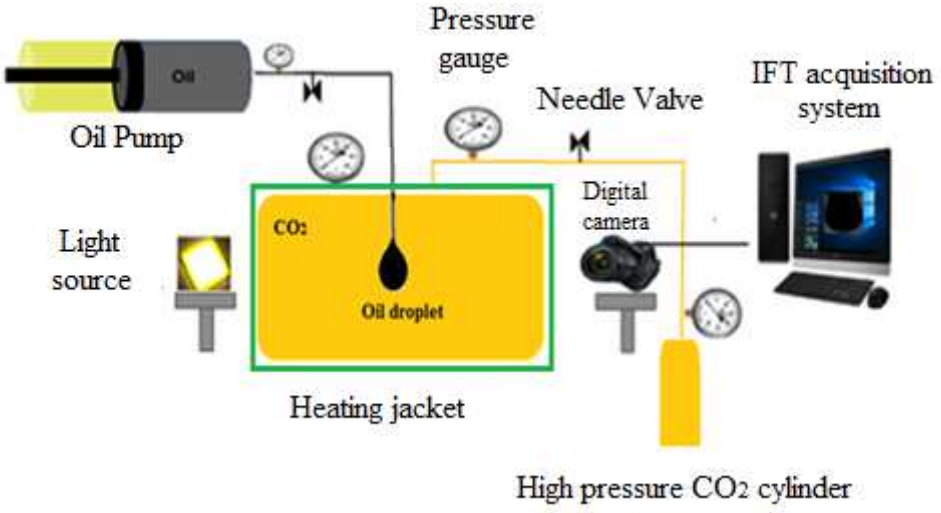

Figure 2. Schematic of high pressure and high temperature interfacial tension for CO_2-oil tests.

2.2.4 Natural depletion tests

Natural depletion tests were performed with static apparatus as Figure 3, and it was used high pressure metal filter with 0.22 micron size. The set up was contain pump for injecting hydraulic fluid below main piston, high pressure and temperature recombined cell, main cell, high pressure 0.22 micron metal filter, cell of fluid sampling, gauges for detecting pressure, and temperature sensor. Below five steps were used for performing natural depletion at static phase:

1. Transferring high pressure crude oil sample through main cell.
2. Stirring the main cell for 24 hours.
3. Opening outlet needle valve and pass the high pressure sample through 0.22 micron metal filter.
4. Obtaining asphaltene content percent with standard IP143 method.
5. Calculation of the asphaltene precipitation with subtracting asphaltene content from step 4 from asphaltene content at initial case.

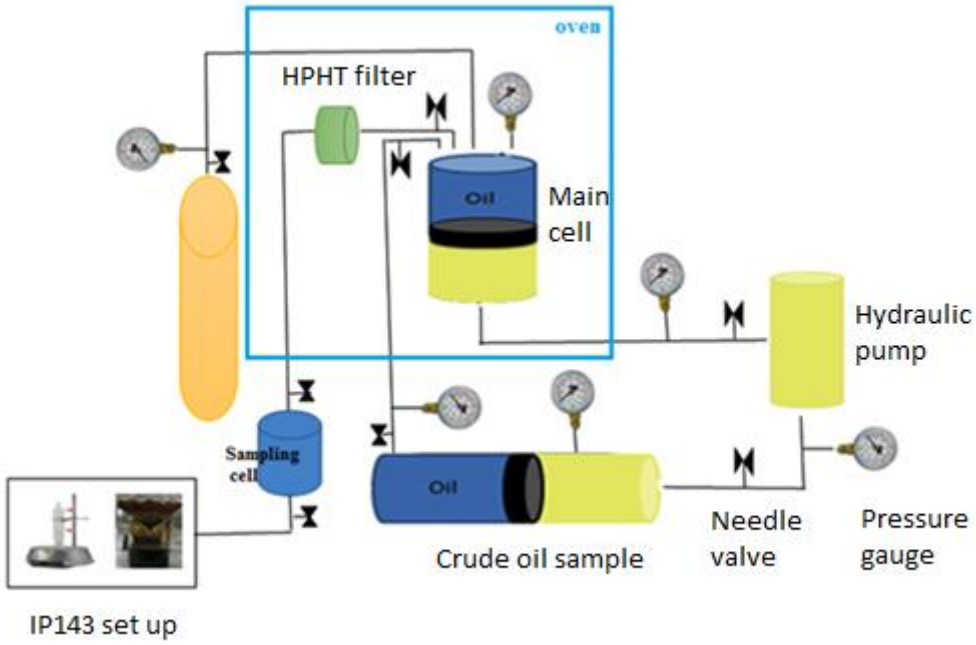

Figure 3. Set up for performing natural depletion.

2.2.5 Batch adsorption experiment

Surveying adsorption of asphaltene on NCs or zeolite nanoparticles surface was performed with Batch adsorption tests with toluene solution. Below five steps were used during this adsorption test:

1. Adding certain amounts of NCs or zeolite's nanoparticles concentration.
2. Shaking solution at 200 rpm for 4 hours [47].
3. Using centrifuge at 3000 ppm and 30 minutes for separating asphaltene which adsorbed on NCs or zeolite nanoparticles surface.
4. Measuring remaining asphaltene concentration.
5. Calculating the amount of adsorbed asphaltene on nanoparticles surface with Equation 1 as below:

$$Q=\frac{(C_o-C_e)}{m}*V \quad (1)$$

The main items in Equation 1 and the relevant units are Initial asphaltene concentration (C_o), mg/L, asphaltene equilibrium concentration(C_e) , mg/L, volume of solution (V), L, NCs mass (m), mg.

2.2.6 Dynamic experimental CO_2 procedure

A dynamic apparatus schematic of set up that used to perform dynamic CO_2 tests is shown in Figure 4.

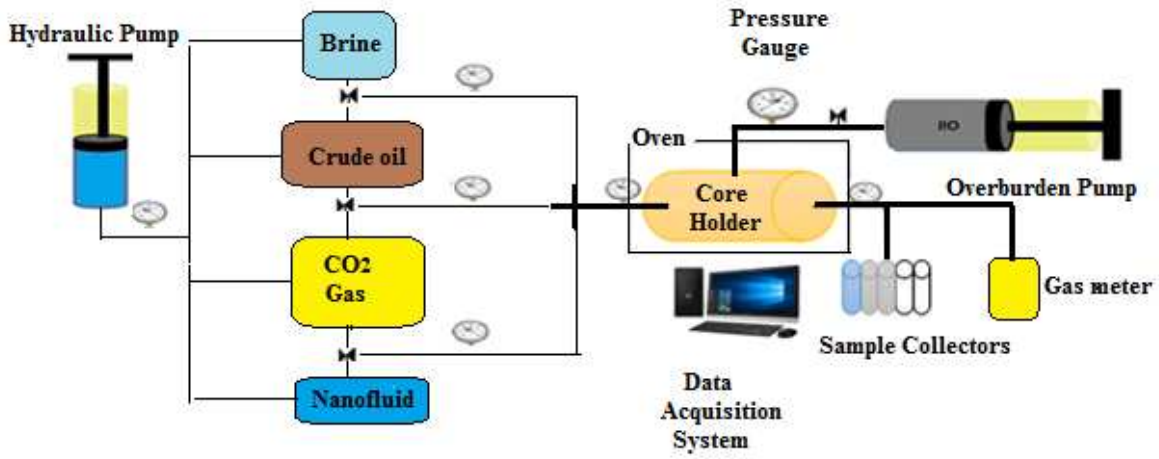

Figure 4. Dynamic apparatus for performing dynamic CO_2 tests.

The dynamic set up was contained three different vessels of brine, nanofluids, and crude oil, hydraulic pump, core holder for holding carbonate core plug, pressure and temperature sensors, overburden pump, DP sensors, and acquisition data. Below five steps were used for performing dynamic CO_2 tests in the presence of NCs:

1. Injecting formation water (0.1 cc/min) and calculate water permeability
2. Obtaining residual water saturation with performing oil injection
3. Calculation of effective oil permeability at residual water saturation
4. Injecting simultaneous oil and CO_2
5. Obtaining permeability reduction

For nanocopmosite, the procedure was same except step 4, which oil contains NCs 30 ppm at 1700 Psi and 40 ℃. Figure 5 shows the experimental approach which was used in this study:

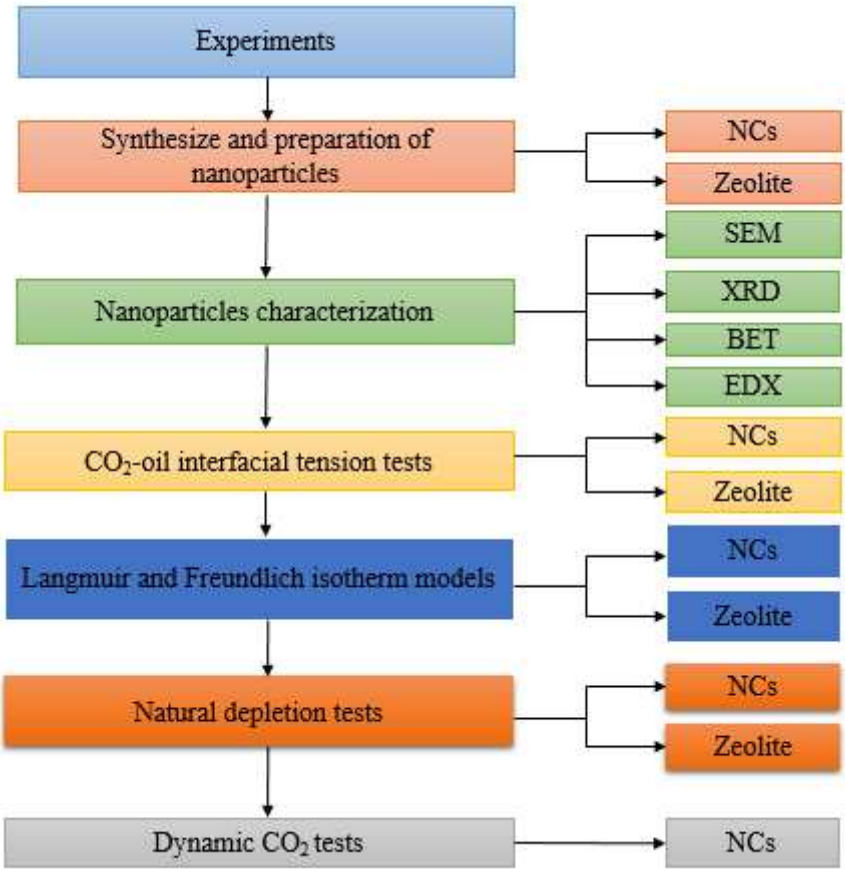

Figure 5. Schematic of experimental procedures.

3. Results and discussion

3.1 Characterization

Figure 6 shows X-ray analysis for detecting the structure of NCs and Zeolite nanoparticles. Zeolite structure is determined through d_{hkl} = 7.5°, 8.5°, 23° and 24° reflections [48-49]. Figure 6b shows Zirconia planes based on the JCPDS 79-1771 ([2θ; planes] are [30.47, 36.78°, 50.17, 60.23, 61.81 and 73.59; 111, 200, 220, 311, 222 and 400]. Moreover, Copper

oxide particles was detected according to Zhu et al group (2θ = 36.12°, 40.82°, 58.61° and 67.38) [50]. Equation 2 was used for determining nanoparticles size:

$$\tau = \frac{k\lambda}{\beta \cos\theta} \qquad (2)$$

τ, *k*, λ, *β*, and *θ* are crystalline size (nm), shape factor (0.9), x-rays wavelength (0.154 nm), line broadening, and Bragg angle. NCs calculated average size was 30.21 nm.

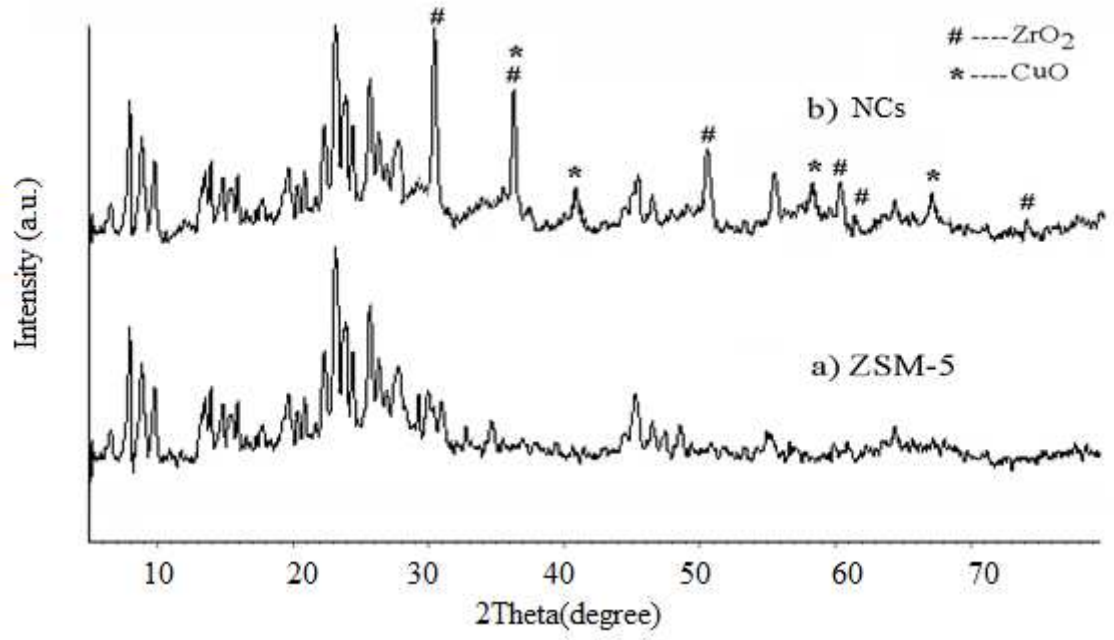

Figure 6. XRD pattern of (a) zeolite and (b) zeolite-zirconia-copper nanocomposites (NCs)

The morphological surface and size of nanoparticles were investigated by SEM. Images obtained from nanozeolite and synthesized zeolite-zirconia-copper nanocomposites (NCs) are shown in Figure 7. As it can be seen from Figure 7a side from morphologically point of view, the zeolite sample is composed of a large number of coffin-shaped units with relatively similar dimensions of about 50 nm. In this image, it is possible to see the uneven surfaces of

the bed and cavities, which will increase the specific surface area and adsorption capacity.With regard to gained SEM image from zeolite-zirconia-copper nanocomposites (NCs) as Figure 7b, it can be observed that the zirconia-copper particles were uniformly distributed at surface of zeolite with dimensions less than 30 nm. This is a sign of the successful stabilization of nanoparticles on the zeolite substrate.

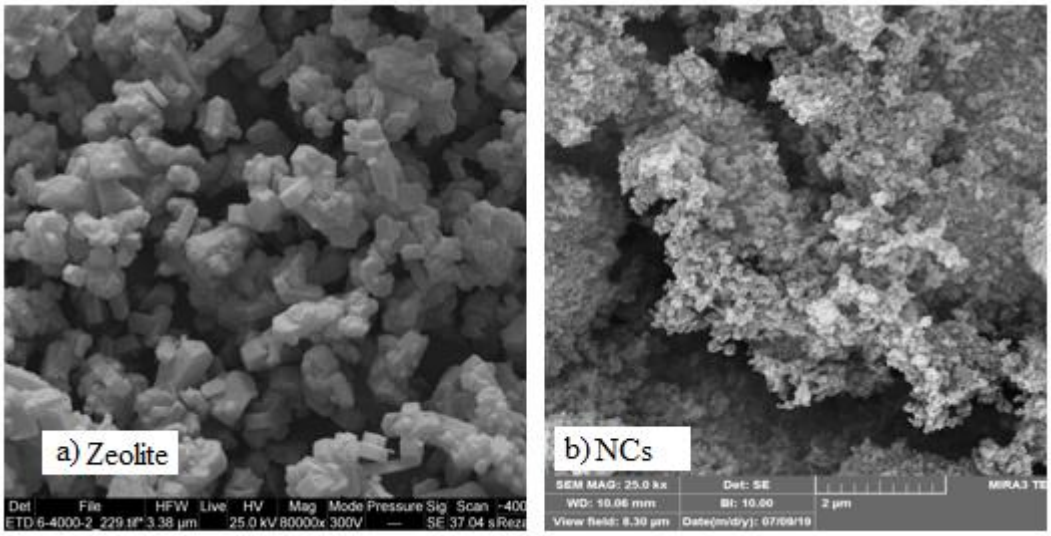

Figure 7. SEM images of a: zeolite and b: zeolite-zirconia-copper nanocomposites.

The surface area, pore size, and pore volume of the pure zeolite and zeolite-zirconia-copper nanocomposites (NCs) were measured by BET. The results are summarized in Table 3. The specific surface areas of the NCs (327.82 m^2/g) is less than the pure zeolite (369.48 m^2/g) as a result of introducing of ZrO_2 and CuO. An increase in the ZrO_2 and CuO contents decreases the specific surface area due to increasing the crystal size and the pore blockage of the support. As compared to NCs, pure zeolite has a higher specific surface area and higher pore volume, but lower average pore diameter.

Table 3. Textural properties of the prepared materials

Sample	Surface area (m^2/g)	Pore volume (cm^3/g)	Average pore diameter (nm)
zeolite	369.5	0.12	1.02
NCs	327.8	0.11	1.22

NCs = Zeolite-zirconia-copper nanocomposites

Figure 8 and Table 4 show EDX results for zeolite nanoparticles and NCs. Figure 8a shows different elements in the zeolite nanoparticles such as Si (31.49), Al (3.38), Na (16.32) and O (48.81) [51]. Different elements of Al, Si, O, and Na were observed in the NCs composition as Figure 8b and Table 4. Zirconia and Copper were observed in zeolite nanoparticles based on EDX images.

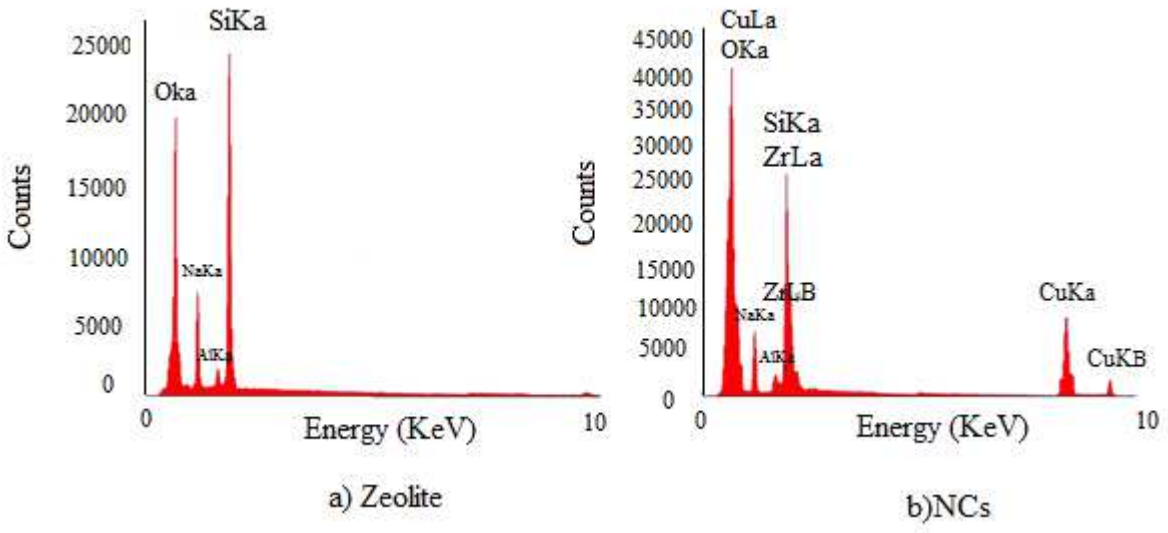

Figure 8. EDX images of a) zeolite (left) and b) Zeolite-zirconia-copper nanocomposites (right).

Table 4. EDX data for zeolite and NCs.

Elements	Atomic percentage (At%)	
	zeolite	NCs
Si	31.49	19.89
Al	3.38	2.44
Na	16.32	6.84
O	48.81	54.91
Zr	---	13.21
Cu	---	4.18

3.2 Asphaltene adsorption isotherms in the presence of NCs and zeolite nanoparticles

Langmuir and Freundlich isotherm models which were used in this study are expressed in Equations 3 and 4 [52].

$$Q_e = Q_m \frac{K_L C_e}{1+K_L C_e} \quad (3)$$

$$Q_e = K_F C_e^{1/n} \quad (4)$$

Equations 5 and 6 are expressed in linear form as:

$$\frac{C_e}{Q_e} = \frac{1}{Q_m K_L} + \frac{Ce}{Q_m} \quad (5)$$

$$\text{Ln } (Q_e) = \text{Ln } (K_F) + \frac{1}{n} \text{Ln } (C_e) \quad (6)$$

Asphaltene adsorption on NCs and zeolite's surface (mg/g), equilibrium concentration of NCs and zeolite (mg/L), maximum asphaltene adsorption per grams of NCs or zeolite (mg/g), Langmuir constant of adsorption, the capacity of adsorption in Freundlich isotherm ([mg/g] [L/mg]), and intensity factor in in Freundlich isotherm were shown with Q_e, Ce, Q_m, K_L, K_F, and 1/n, respectively. Figure 9 shows asphaltene adsorption on the NCs nanocomposites and zeolite's surface in the batch experiment tests up to 1000 ppm. As it is clear from the graph, there is two different slope below 100 ppm and after that. At first slope (below 100 ppm), the slope was dramatically increased. Then after, asphaltene adsorption on the NCs

nanocomposites and zeolite's surface was reached to around 78.5 mg/g, and 33 mg/g, respectively. Accordingly NCs was adsorbed more asphaltene on its surface in compared to zeolite nanoparticles. It was concluded from previous research that the type of sorbent is affected on the amount and type of adsorption [53-55]. According to the isotherm model results in this study, the adsorption data was adapted well with Langmuir isotherm than Freundlich isotherm, and this shows that adsorption surface was monolayer and homogeneous. Freundlich isotherm occurs in the surface that has different energy with heterogeneous surface [55], and from the comparison between Freundlich isotherm between zeolite and NCs, it was observed that the data less adopted with NCs in comparison zeolite. Langmuir and Freundlich isotherm linear plots were shown in Figures 10 and 11, respectively.

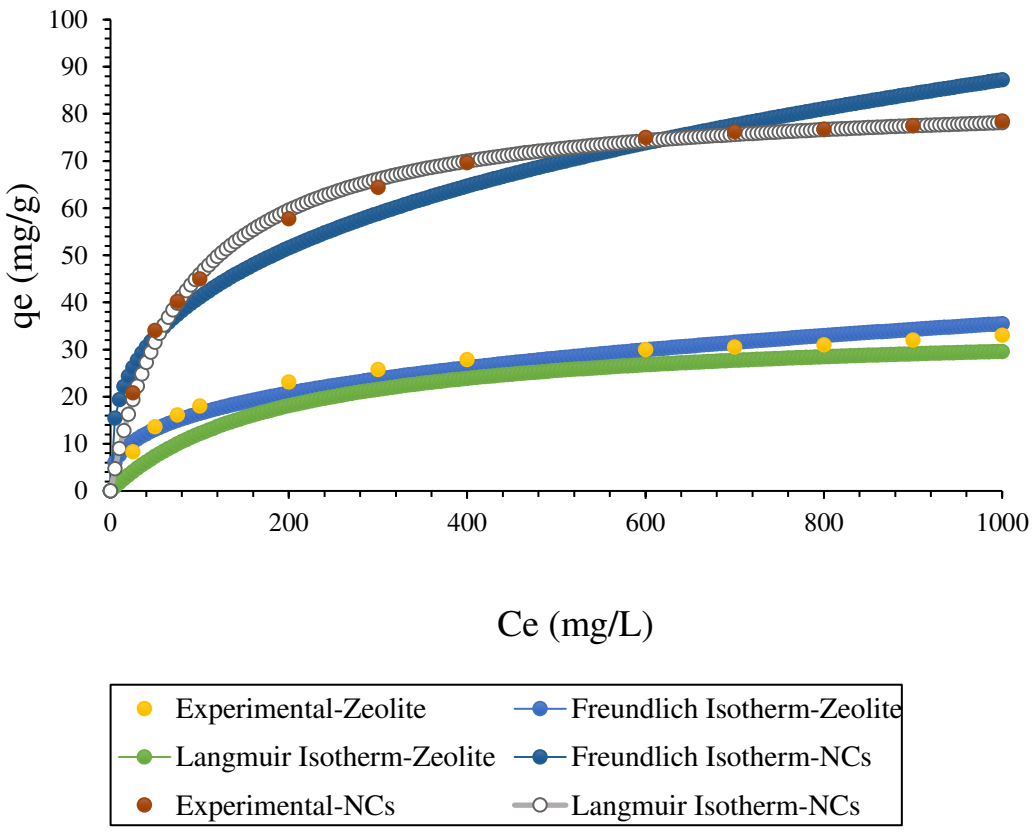

Figure 9. Asphaltene adsorption models (Langmuir and Freundlich) for NCs and zeolite nanoparticles.

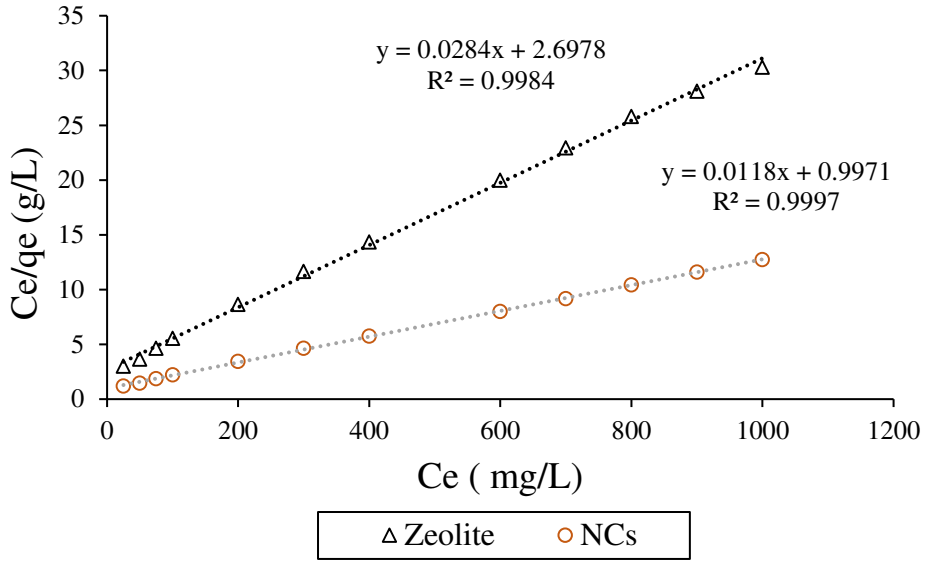

Figure 10. Langmuir model constants for NCs and zeolite nanoparticles.

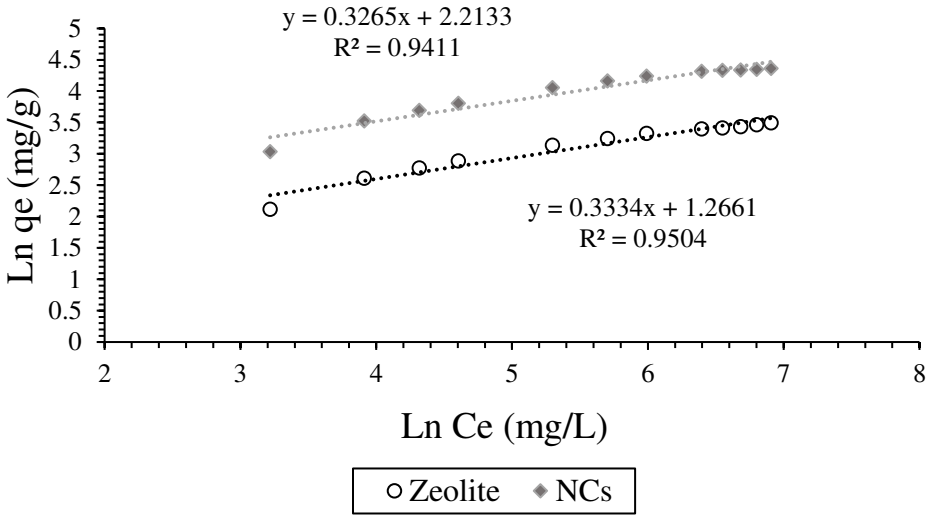

Figure 11. Freundlich model constants for NCs and zeolite nanoparticles.

Isotherm parameters of both isotherm models were shown in Table 5. According to the results, NCs has better adsorption capacity in comparison to the zeolite nanoparticles. The maximum adsorption ratio of NCs to the zeolite (Q_m NCs/Q_m zeolite) was 2.41. Furthermore, NCs had higher adsorption capacity in comparison zeolite, and the K_F NCs / K_F zeolite was 2.5782.

Table 5. Langmuir and Freundlich isotherm model constants.

Nanoparticles	Langmuir			Freundlich		
	q_m [mg/g]	K_L (L/mg)	R^2	1/n	K_F [mg/g][L/mg]	R^2
NCs	84.7458	0.01181	0.9997	0.3265	9.1437	0.9411
Zeolite nanoparticles	35.2113	0.01052	0.9984	0.3334	3.5465	0.9504

3.3 Effect of nanoparticles concentration and pressure on CO_2-crude oil interfacial tension

The effects of NCs and zeolite nanoparticles on the CO_2-Oil IFT was shown in Figures 12. According to the results, there are two different ranges from 200-2600 Psi. Interfacial tension of CO_2-Oil was decreased due to dissolving CO_2 in the crude oil. The slope in this graph was changed due to forming the aggregate of asphaltene particles. According to the Figure 12, NCs was changed the slope in the second region more than Na-ZSM-5 zeolite, and in other words adsorbed higher amounts of asphaltene on its surface. As it was mentioned in the previous section, NCs had the better asphaltene adoption in comparison to zeolite nanoparticles which confirmed with this results. Moreover, one of the other important results from the results was delaying agglomeration in the presence of NCs and zeolite nanoparticles, and it was confirmed that NCs had better results in this aspect as well that zeolite. Previously Kazemzadeh et al was seen same results in the presence of Fe_3O_4 nanoparticles [56]. Seven pressures from the second region (1700-2600 Psi) were selected for obtaining the relation between these high adsopber points with adsorption in the real crude oil in natural depletion tests.

As it was mentioned, there are two different slope of CO_2-Oil in the base and both nanoparticles of NCs and zeolite, and Table 6 summarized different equations in these two region. 2nd to 1st slope ratio was 19.697 % at base case, and 2nd to 1st ratio increased to 20.895 % and 29.851 % in the presence of NCs and zeolite at 30 ppm, respectively. Thus, NCs had better performance with regards adsorbing asphaltene on its surface in comparison zeolite.

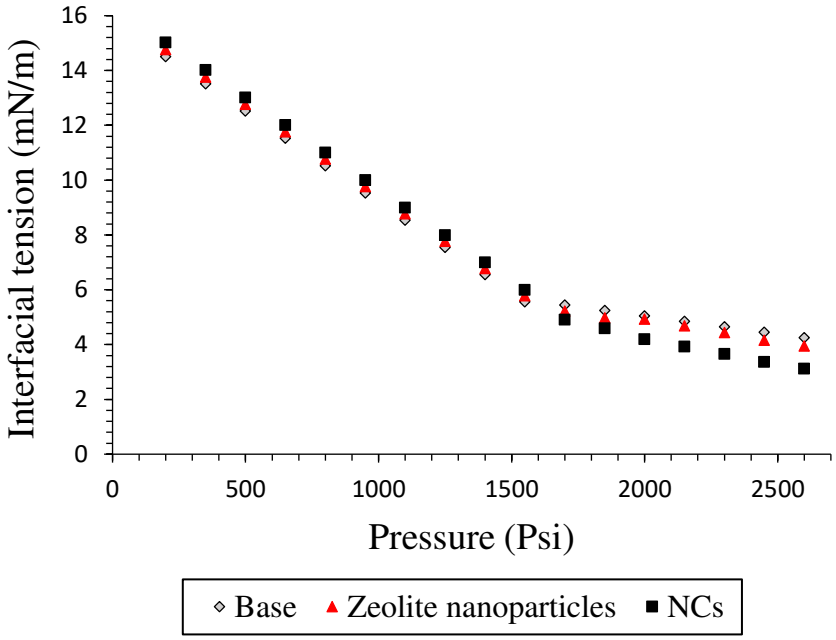

Figure 12. Effects of pressure and nanoparticles (NCs and zeolite) on CO_2 - oil IFT.

Table 6. Changes in CO_2-oil IFT slope ratio in the presence of NCs and zeolite nanoparticles.

Nanoparticles type	Nanoparticle concentration (ppm)	Region	Equation IFT (mN/m)	Ratio of the IFT slope in 2nd to the 1st region (%)
Base	-	1:(200-1550)Psi	IFT= -0.0066P + 15.823	19.697
		2:(1700-2600)Psi	IFT = -0.0013P + 7.6943	
Zeolite nanoparticles	30	1:(200-1550)Psi	IFT = -0.0067P + 16.353	20.895
		2:(1700-2600)Psi	IFT = -0.0014P + 7.6647	
NCs	30	1:(200-1550)Psi	IFT= -0.0067P + 16.088	29.851
		2:(1700-2600)Psi	IFT= -0.0020P + 8.2414	

3.4 Natural depletion tests in the presence of nanoparticles

As it was mentioned in the previous section, seven pressure of 1700, 1850, 2000, 2150, 2300, 2450, and 2600 Psi have selected as high adsorption points for static phase and performing natural depletion tests in the presence of NCs and zeolite nanoparticles. Asphaltene precipitation content versus pressures at static pressure were shown in Figure 13, and effects of both NCs and zeolite nanoparticles were observed according to this graph. It was seen asphaltene precipitation of NCs and zeolite nanoparticles decreased from (5.10 wt%, 14.34 wt %) to (3.78 wt%, 8.40 wt %) and (2.8 wt%, 6.25 wt %), respectively during pressure reduction from 2600 Psi to 1700 Psi. Accordingly, based on the results, NCs had better results for decreasing asphaltene precipitation in the static phase in comparison to zeolite, and it can be in a direct relation with higher adsorption potential in the previous steps.

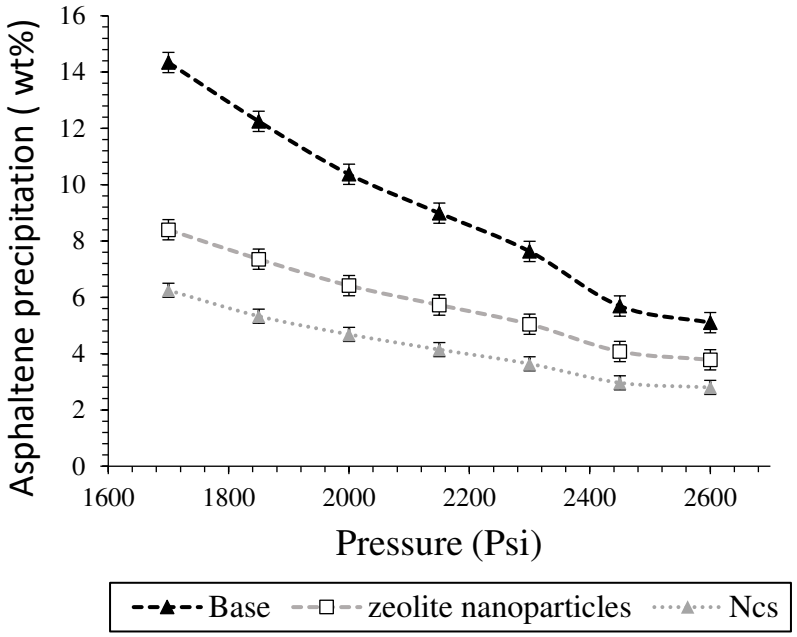

Figure 13. Effects of NCs and zeolite nanoparticles on asphaltene precipitation during natural depletion tests.

3.5 Dynamic CO_2 tests in the presence of NCs

According to the static phase results, NCs had better results than zeolite in aspect of asphaltene adsorption and asphaltene precipitation reduction. Thus it was selected for surveying permeability/porosity reduction parameters. As it is clear from the Table 7, NCs had better results in lower pressure for asphaltene precipitation at 1700 Psi, 1700 Psi, 40 ℃, and 30 ppm were selected for performing CO_2 flooding at dynamic phase.

Table 7. Difference between Initial asphaltene precipitation and asphaltene precipitation in the presence of NCs.

Pressure	Initial asphaltene precepitation	Asphaltene precepitation in the presence of NCs	(Initial-NCs) asphaltene precipitation
Psi	Wt %	Wt %	Wt %
1700	14.34	6.25	8.09
1850	12.25	5.33	6.92
2000	10.37	4.68	5.69
2150	8.99	4.14	4.85
2300	7.63	3.63	4.00
2450	5.69	2.96	2.73
2600	5.10	2.80	2.30

One of the important factor in porous media is considering deposition condition. As it was shown in the static phase, NCs had better performance in comparison to zeolite. Accordingly it was selected for surveying its effect on the deposition rate in porous media. Dynamic

displacement tests were used for CO_2 flooding in the presence of NCs. As it is clear from the Figure 14, asphaltene deposition in the presence of gas was increased during CO_2 flooding. By measuring the asphaltene content of injected and produced oil samples, one can estimate the amount of deposition in porous media. The asphaltene of produced oil was measured by IP143 standard technique. After adding NCs in crude oil, asphaltene precipitation was decreased. As CO_2 gas volume was increased from 1 to 6 pore volume, asphaltene precipitation (Wt %) was decreased from (15.12, 18.12) to (11.85, 14.44), respectively.

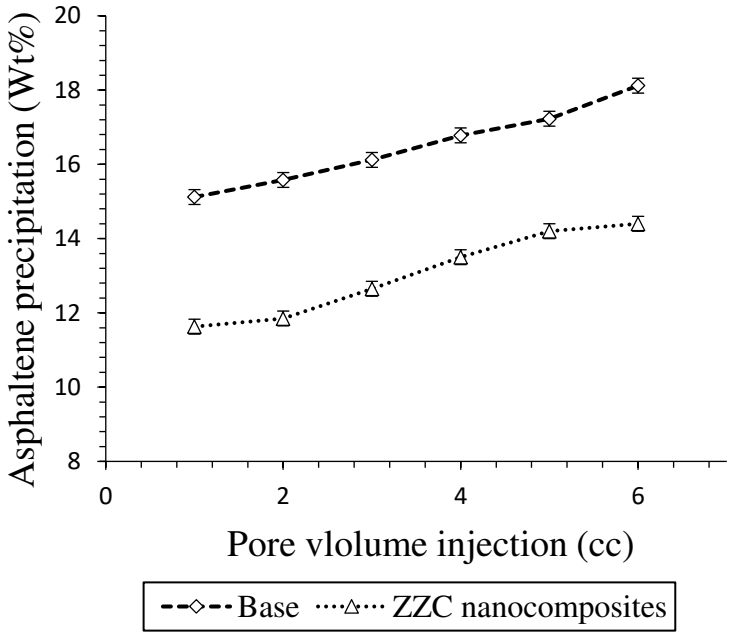

Figure 14. Effect of NCs on the asphaltene deposition during CO_2 flooding.

As it was mentioned before, after saturation of carbonate core sample with brine, recombined oil and CO_2 [25 Mole % which was more than initial onset value (20 Mole %) at static phase] displaced through the low permeability carbonate core and initial permeability reduction was recorded. Then, same procedure was performed in the presence of NCs [dispersed in oil] at 30 ppm, 1700 Psi, and 40 ℃ as Figure 15 and 16. Many other cases and laboratory studies have been reported on precipitation and deposition of asphaltenes in porous media during immiscible or miscible gas flooding operations [57-63]. Figure 15 shows permeability

reduction in the presence of NCs, and based on the results, NCs improved permeability reduction in porous media. Figure 16 shows differential pressure between inlet and outlet of cores for both tests. As it is clear from the graph, most of pressure drop was occurs at initial part which asphaltene deposition problem was serious at this point. Moreover, NCs decreased pressure drop successfully in comparison to base CO_2 flooding.

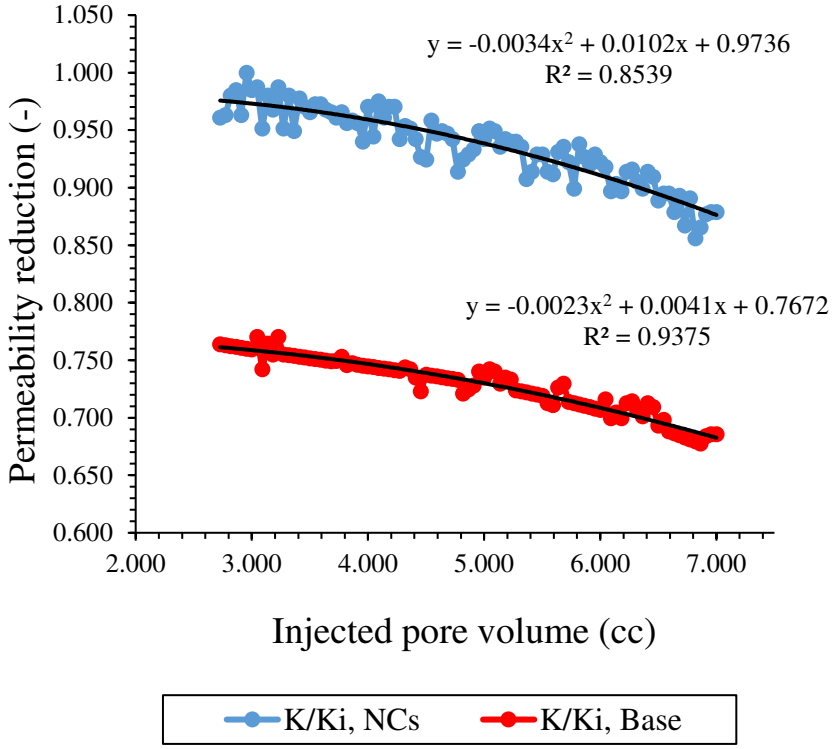

Figure 15. Permeability reduction in the presence of NCs during CO_2 flooding.

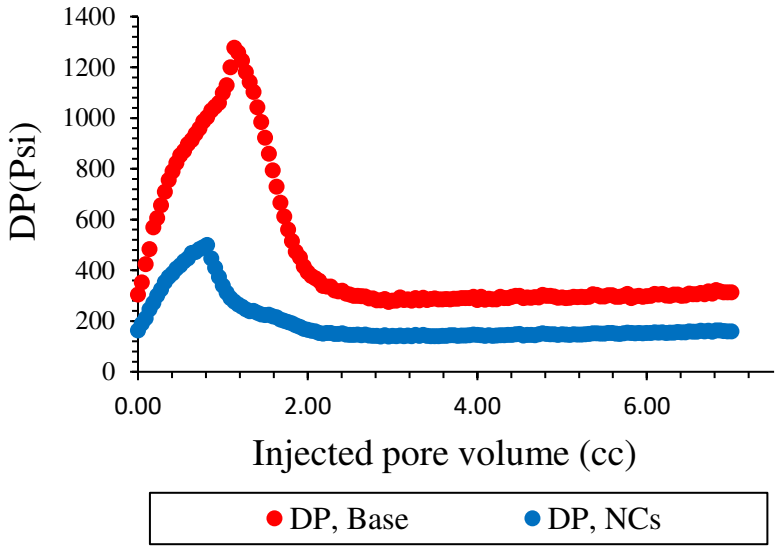

Figure 16. Differential pressure in the presence of NCs during CO_2 flooding.

There is direct relation between porosity reduction and asphaltene deposition rate. Figure 18 shows the porosity variations of low permeability carbonate reservoir versus the amounts of pore volume. As it was observed in the previous steps, NCs was decreased asphaltene precipitation in static phase at 30 ppm, and at same concentration asphaltene deposition was decreased in carbonate reservoir. Moreover, higher porosity reduction was seen at higher asphaltene deposition points.

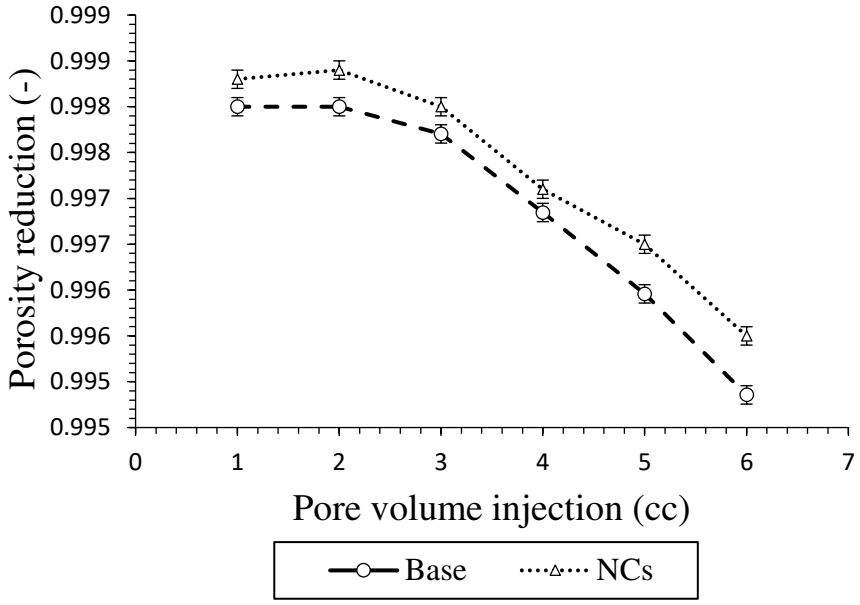

Figure 17. Porosity reduction in the presence of NCs during CO_2 flooding.

Conclusions

Zeolite-zirconia-copper oxide nanocomposites (NCs) has been synthesized successfully with average size of 30 nm and it was used for asphaltene adsorption and solving asphaltene precipitation problems and the results compared with zeolite nanoparticles. Results show that NCs nanoparticles adsorbed higher amount of asphaltene and asphaltene precipitation decreased more in the presence of NCs nanoparticles than zeolite nanoparticles which reveals this point that this nanocomosites can be used efficiently as an asphaltene inhibitor and the agglomeration process was delayed efficiently. Adsorption data fitted well with the Langmuir model in comparison to the Freundlich model, which shows that the adsorption occurs in a homogeneous surface with monolayer coverage in the presence of both nanoparticles. Based on the BET results, NCs has lower surface area, higher pore volume but higher diameter in comparison to zeolite nanoparticles. EDX analysis confirmed that NCs synthesized successfully. There is two different slope in CO_2-oil IFT readings as pressure increased (200 Psi-2600 Psi), and second slope is slower than the first one which is due to aggregation of asphaltene. Seven pressures of 1700, 1850, 2000, 2150, 2300, 2450, 2600 Psi and NCs and zeolite nanoparticles at concentration of 30 ppm were selected for performing natural depletion tests and it was concluded that as pressure decreased from (2600 Psi to 1700 Psi), asphaltene precipitation in the presence of NCs and zeolite decreased from (Base: 5.10 wt%, 14.24 wt%) to (2.80 wt%, 6.25 wt%) and (3.78 wt%, 8.40 wt%), respectively. It was observed that the NCs has higher efficiency with regards adsorbing asphaltene on its surface and decreasing asphaltene precipitation during natural depletion in comparison to zeolite nanoparticles, and and it was selected for performing CO_2 dynamic tests. In dynamic phase. It was observed that NCs had high potential material for improving permeability impairment, porosity reduction, and asphaltene deposition rate during CO_2 flooding tests.

References

[1] Kralova, I., Sjöblom, J., Øye, G., Simon, S., Grimes, B. A. and Paso, K. Heavy crude oils/particle stabilized emulsions', Adv. Colloid Interface Sci, 2011, 169, 2, 106-127. DOI:10.1016/j.cis.2011.09.001.

[2] Östlund, J. A., Wattana, P., Nydén, M. and Fogler, H. S. Characterization of fractionated asphaltenes by UV–vis and NMR self-diffusion spectroscopy, J. Colloid Interface Sci, 2004, 271, 2, .372-380. DOI: 10.1016/j.jcis.2003.10.033.

[3] Yarranton, H. W., Alboudwarej, H. and Jakher, R. Investigation of Asphaltene Association with Vapor Pressure Osmometry and Interfacial Tension Measurements, Ind. Eng. Chem. Res., 2000, 39, 8, 2916–2924. DOI: 10.1021/ie000073r.

[4] Hemmati-Sarapardeh, A., Alipour-Yeganeh-Marand, R., Naseri, A., Safiabadi, A., Gharagheizi, F., Ilani- Kashkouli, P. and Mohammadi, A. H. Asphaltene precipitation due to natural depletion of reservoir: Determination using a SARA fraction based intelligent model', Fluid Phase equilibria, 2013, 354, 177–184. DOI: 10.1016/j.fluid.2013.06.005.

[5] Rudyk, S. and Spirov, P. Upgrading and extraction of bitumen from Nigerian tar sand by supercritical carbon dioxide. Al, Energy, 2014,113, 1397–1404. DOI: 10.1016/j.apenergy.2013.08.076.

[6] Thawer, R., Nicoll, D. C. A. and Dick, G. Asphaltene deposition in production facility, SPE Prod. Eng, 1990, 5, 475–480. DOI: 10.2118/18473-PA.

[7] Valter Antonio, M. B., Mansoori, G. A., De Almeida Xavier, L. C.; Park, S. J. and Manafi, H. Asphaltene flocculation and collapse from petroleum fluids, J. Pet. Sci. Eng, 2001, 32, 217–230. DOI: 10.1016/S0920-4105(01)00163-2.

[8] Karimi, A., Fakhroueian, Z., Bahramian, A., Khiabani, N. P., Darabad, J. B., Azin, R. and Arya S. Wettability alteration in Carbonates using Zirconium Oxide Nanofluids: EOR Implications', Energy Fuels, 1991,26, 2, 1028-1036. DOI: 10.1021/ef201475u.

[9] Trbovich, M. G. and King, G. E. Asphaltene Deposit Removal: Long-Lasting Treatment with a Co-Solvent, Paper SPE-21038-MS Presented at the SPE International Symposium on Oilfield Chemistry, 1991, 20-22 February 1991. Anaheim, California, USA. DOI: 10.2118/21038-MS.

[10] Naghdi, N. and Mirzayi, B. Adsorption and Removal of Asphaltene Using Synthesized Maghemite and Hematite Nanoparticles, Energy Fuels, 2015, 29, 3, 1397–1406. DOI: 10.1021/ef502494d

[11] Franco, C. A., Montoya, T., Nassar, N. N., Pereira-Almao, P. and Cortes, F. B. Adsorption and Subsequent Oxidation of Colombian Asphaltenes onto Nickel and/or Palladium Oxide Suorted on Fumed Silica Nanoparticles, Energy Fuels, 2013, 27, 12, 7336-7347. DOI: 10.1021/ef4000825.

[12] Hashemi, R., Nassar, N. N. and Pereira-Almao, P.Transport behavior of multi metallic ultra-dispersed nanoparticles in an oil-sands-packed bed column at a high temperature and pressure', Energy Fuels, 2012, 26, 3, 1645-1655. DOI: 10.1021/ef201939f

[13] Nassar, N. N., Hassan, A. and Pereira-Almao, P. Metal oxide nanoparticles for asphaltene adsorption and oxidation'. Energy Fuels, 2011, 25, 3, 1017-1023.

[14] Olvera, J. N. R., Gutierrez, G. J., Serrano, J.,Ovando, A. M., Febles, V. G. and Arceo, L. D.

B. Use of unsuorted, mechanically alloyed NiWMoC nanocatalyst to reduce the viscosity of aquathermolysis reaction of heavy oil. Catalysis Communications, 2014, 43, 131-135.

[15] Hashemi, R., Nassar, N. N. and Pereira-Almao, P. R. In situ Upgrading of Athabasca Bitumen Using Multimetallic Ultra-Dispersed nanocatalysts in an Oil-Sands-Packed Bed Column: Part 1, Produced Liquid Quality Enhancement, Energy & Fuels, 2013, 28, 2, 1338–1350.

[16] Pernyeszi, T., Patzkó, Á., Berkesi, O. and Dékány, I. Asphaltene adsorption on clays and crude oil reservoir rocks, Colloids Surf, 1988, 137, 3, 373-384.

[17] Bantignies, J. L., Cartier dit Moulin, C. and Dexpert, H. Asphaltene adsorption on kaolinite characterized by infrared and X-ray absorption spectroscopies, J. Pet. Sci. Eng,1988, 20, 4,233-237.

[18] Pernyeszi, T. and Dékány, I. Sorption and elution of asphaltenes from porous silica surfaces, Colloids Surf, A, 2001, 194, 25-39.

[19] Balabin, R. M., Syunyaev, R. Z., Schmid, T., Stadler, J., Lomakina, E. I. and Zenobi, R. Asphaltene Adsorption onto an Iron Surface: Combined Near-Infrared (NIR), Raman, and AFM Study of the Kinetics, Thermodynamics, and Layer Structure'. Energy Fuels, 2011, 25, .189-196.

[20] Nassar, N. N. Asphaltene adsorption onto alumina nanoparticles: kinetics and thermodynamic studies, Energy Fuels, 2010, 24, 8, 4116-4122.

[21] Nassar, N. N., Hassan, A. and Pereira-Almao, P. Effect of surface acidity and basicity of aluminas on asphaltene adsorption and oxidation, J. Colloid Interface Sci., 2011,360, 1, 233-238.

[22] Franco, C., Patiño, E., Benjumea, P., Ruiz, M. A. and Cortés, F. B. Kinetic and thermodynamic equilibrium of asphaltenes sorption onto nanoparticles of nickel oxide suorted on nanoparticulated alumina'. Fuel, 2013, 105, 408-414.

[23] Alboudwarej, H., Pole, D., Svrcek, W. Y. and Yarranton, H. W. Adsorption of asphaltenes on metals', Ind. Eng. Chem. Res., 2005,44, 15, 5585-5592.

[24] Nassar N. N., Hassan A., Pereira-Almao P. Metal oxide nanoparticles for asphaltene adsorption and oxidation, Energy Fuels, 2011, 25, 3, 1017-1023.

[25] Nassar N. N., Hassan A., Pereira-Almao P. Effect of surface acidity and basicity of aluminas on asphaltene. J Colloid Interface Sci, 2011, 360, 1, 233-8. doi:10.1016/j.jcis.2011.04.056.

[26] Kosinov, N., Liu, C., Hensen, E. J., Pidko, E. A., Engineering of transition metal catalysts confined in zeolites. Chem. Mate, 2018, 30, 3177–3198.

[27] He, Y. Zeolite supported Fe/Ni bimetallic nanoparticles for simultaneous removal of nitrate and phosphate: synergistic effect and mechanism. Chemical Engineering Journal, 2018, 347, 669–681.

[28] Hosseinpour, N., Khodadadi, A. A., Bahramian, A., and Mortazavi, Y. Asphaltene Adsorption onto Acidic/Basic Metal Oxide Nanoparticles toward in Situ Upgrading of Reservoir Oils by Nanotechnology, Langmuir, 2013, 29, 14135−14146. Doi: 10.1021/la402979h.

[29] Mohammadi, M., Akbari, M., Fakhroueian, Z., Bahramian, A., Azin, A., and Arya, S. Inhibition of Asphaltene Precipitation by TiO_2, SiO_2, and ZrO_2 Nanofluids, Energy Fuels 2011, 25, 3150–3156.

[30] Zhou, L. Zhao, Q. Huang, R. Zhou and X. Li. Catalytic Activity of Y Zeolite Suorted CeO_2 Catalysts for Deep Oxidation of 1, 2-Dichloroethane (DCE), Cat. Lett, 2009, 127, 277-284.

[31] Zheng, X. Zhang, S. Wang, Wang, X., and Wu, S. Effect of Addition of Base on Ceria and Reactivity of CuO/CeO_2 Catalysts for Low Temperature CO Oxidation, J. Natural Gas Chem. 2007, 16, 179-185

[32] Strobel, C., Förster, M., Hilger, I. Biocompatibility of cerium dioxide and silicon dioxide nanoparticles with endothelial cells, Journal of Nanotechnology, 2014, 5, 1795-1807.

[33] Alswata, A. A., Ahmad, M. B., Al-Hada, N. M., Kamari, H. M., Hussein, M. Z. B., Ibrahim, N. A. Preparation of zeolite/zinc oxide nanocomposites for toxic metals removal from water. Results in Physics, 2017, 7, 723-731.

[34] Dong, J., Tian, T., Ren, L., Zhang, Y., Xu, J., Cheng, X. CuO nanoparticles incorporated in hierarchical MFI zeolite as highlyactiveelectrocatalyst for non-enzymatic glucose sensing Colloids and Surfaces B: Biointerfaces, 2015, 125, 206-212.

[35] Verma, M., Tyagi, I., Chandra, R., Gupta, V. K. Adsorptive removal of Pb(II) ions from aqueous solution using CuO nanoparticles synthesized by sputtering method, J. Mol. Liq., 2017, 225, 936–944.

[36] Mahdavi, S., Jalali, M., Afkhami, A. Removal of heavy metals from aqueous solutions using Fe3O4, ZnO, and CuO nanoparticles, J. Nanopart. Res., 2012, 14, 171–188.

[37] Chakraborty, A., Islam, D. A., Acharya, H. Facile synthesis of CuO nanoparticles deposited zeolitic imidazolate frameworks (ZIF-8) for efficient photocatalytic dye degradation, J. Solid State Chem., 2019, 269, 566–574.

[38] Kim, J. W., Ki, C. S., Um, I. C., Park, Y. H. A facile fabrication method and the boosted adsorption and photodegradation activity of CuO nanoparticles synthesized using a silk fibroin template, J. Ind. Eng. Chem., 2017, 56, 335–341.

[39] Gupta, V. K., Chandra, R., Tyagi, I., Verma, M. Removal of hexavalent chromium ions using CuO nanoparticles for water purification applications, J. Colloid Interface Sci., 2016, 478, 54–62.

[40] Nuengmatcha, P., Porrawatkul, P., Chanthai, S., Sricharoen, P., Limchoowong, N. Enhanced photocatalytic degradation of Methylene blue using Fe_2O_3/graphene/CuO nanocomposites under visible light, J. Environ. Chem. Eng., 2019, 7, 103438.

[41] Manan, M., Farad, S., Piroozian, A., Esmail, M. Effects of nanoparticle types on carbon dioxide foam flooding in enhanced oil recovery.Pet. Sci. Technol.2015, 33, 1286–1294.

[42] Yahya, N., Kashif, M., Nasir, N., Niaz Akhtar, M., Yusof, N. M. Cobalt ferrite nanoparticles: An innovativeapproach for enhanced oil recovery application.J. Nano Res, 2012, 17, 115–126.

[43] Pillewan, P., Mukherjee, S., Roychowdhury, T., Das, S., Bansiwal, A., Rayalu, S. Removal of As (III) and As (V) from water bycopper oxide incorporated mesoporous alumina. J. Hazard Mater, 2011,186, 367–375.

[44] Hayashi, Y., Okabe, H., Experimental Investigation of Asphaltene Induced Permeability Reduction, Paper presented at the SPE EOR Conference at Oil & Gas West Asia, Muscat, Oman, April 2010. Paper Number: SPE-129271-MS. https://doi.org/10.2118/129271-MS.

[45] Camargo, P. H. C., Satyanarayana, K. G., and Wypych, F. Materials Research, Nanocomposites: synthesis, structure, properties and new application opportunities, 2009, 12, 1-39.

[46] ASTM D6560-17, Standard Test Method for Determination of Asphaltenes (Heptane Insolubles) in Crude Petroleum and Petroleum Products, ASTM International, West Conshohocken, PA, 2017, www.astm.org, 2005.

[47] Kashefi, S., Lotfollahi1, M. N. and Shahrabadi, A. Investigation of Asphaltene Adsorption onto Zeolite Beta Nanoparticles to Reduce Asphaltene Deposition in a Silica Sand Pack', Oil & Gas Science and Technology - Rev. IFP Energies nouvelles, 2018, 73, 2.

[48] Shams-Ghahfarokhi, Z., Nezamzadeh-Ejhieh, A., As-synthesized ZSM-5 zeolite as a suitable support for increasing the photoactivity of semiconductors in a typical photodegradation process. Materials Sciencein Semiconductor Processing, 2015, 39, 265–275

[49] Wang, P., Shen, B., Shen, D., Peng, T., Gao, J. Synthesis of ZSM-5 Ze-olite from Expanded Perlite/Kaolin and its Catalytic Performance for FCC Naphtha Aromatization, Catal. Commun, 2007, 8, 1452–1456.

[50] Zhu, D., Wang, L., Yu, W., Xie, H., Intriguingly high thermal conductivity increment for CuO nanowires contained nanofuids with low viscosity, SCiEntifiC REPORts, 2018, 8, 52-82. DOI: 10.1038/s41598-018-23174-z.

[51] Rostami, S., Azizi, S. N., Ghasemi, S., Preparation of an efficient electrocatalyst for oxalic acid oxidation based on Ag-doped ZSM-5 nanozeolites synthesized from bagasse, Journal of Electroanalytical Chemistry 2017, 788, 235-245.

[52] Nassar, N. N., Hassan, A., Pereira Almao P., Thermogravimetric studies oncatalytic effect of metal oxide nanoparticles on asphaltene pyrolysis under inert conditions, Thermal Analysis and Calorimetry, 2011, 110, 1327-1332.

[53] Syunyaev, R. Z., Balabin, R. M., Akhatov, I. S., Safieva, J. O., Adsorption of petroleum asphaltenes onto reservoir rock sands studied by near-infrared (NIR) spectroscopy, Energy Fuels, 2009, 23, 1230-1236.

[54] Balabin, R. M., Syunyaev, R. Z., Schmid, T., Stadler, J., Lomakina, E. I. and Zenobi, R. Asphaltene Adsorption onto an Iron Surface: Combined Near-Infrared (NIR), Raman, and AFM Study of the Kinetics, Thermodynamics, and Layer Structure, Energy Fuels, 2011, 25, .189-196.

[55] Simon, S. Jestin, J., Palermo, T. and Barre, L. Relation between solution and interfacial properties of asphaltene aggregates, Energy Fuels, 2009, 23, 306-313.

[56] Kazemzadeh, Y., Malayeri, M. R, Riazi, M. and Parsaei, R. Impact of Fe_3O_4 nanoparticles on asphaltene precipitation during CO_2 injection, Journal of Natural Gas Science and Engineering, 2015, 22, 227-234

[57] Bennion, D. B., and Tomas, F. B. The use of carbon dioxide as an enhanced recovery agent for increasing heavy oil production. The Joint Canada/Romania Heavy Oil Symposium. Sinla, Romania, March 7–13, 1993.

[58] Abdulrazag, Y., Zekri., Shedid, A. S. The effect of fracture characteristics on reduction of permeability by asphaltene precipitation in carbonate formation. J. Pet. Sci. Eng 2004, 42, 171–182.

[59] Koka, J. S., Najman, J., Sayegh, S. G., and George, A. Asphaltene precipitation during enhanced recovery of heavy oils by gas injection. CIM/AOSTRA Paper 91-10, CIM/AOSTRA Technical Conference, Banff, Canada, April 21–24, 1991.

[60] Hansen, P. W. A CO_2 tertiary recovery pilot, Little Creek, Mississippi. SPE 6747, SPE Annual Technical Conference and Exhibition, Denver, CO, October 9–12, 1977.

[61] Stalkup, F. I. Carbon dioxide miscible flooding, past, present and the outlook for future. J. Petrol. Tech. Aug: 1102–1112, 1978.

[62] Harvey, M. F., Shelton, L. J., and Kelin, C. H. Field injectivity experiences will miscible recovery projects using alternate rich gas and water injection. J. Petrol. Tech, 1977, 1051–1055.

[63] Mirzayi, B.,Vafaie-Sefti, M., Mousavi-Dehghani, S. A., Fasih, M., Mansoori, G. A. The Effects of Asphaltene Deposition on Unconsolidated Porous Media Properties during Miscible Natural Gas Flooding, Petroleum Science and Technology, 2008, 26, 231-243, DOI: 10.1080/10916460600806143.